Generation of two-color polarization-entangled optical beams with a self-phase-locked two-crystal optical parametric oscillator

Julien Laurat,[1] Gaëlle Keller,[2] Claude Fabre,[2] and Thomas Coudreau[2,3,*]
[1]*Norman Bridge Laboratory of Physics 12-33, California Institute of Technology, Pasadena, California 91125, USA*
[2]*Laboratoire Kastler Brossel, Université Pierre et Marie Curie, Case 74, 4 Place Jussieu, 75252 Paris cedex 05, France*
[3]*Laboratoire Matériaux et Phénomènes Quantiques, Université Denis Diderot, Case 7021, 2 Place Jussieu, 75251 Paris cedex 05, France*
(Received 4 November 2005; published 24 January 2006)

A device to generate polarization-entangled light in the continuous-variable regime is introduced. It consists of an optical parametric oscillator with two type-II phase-matched nonlinear crystals orthogonally oriented, associated with birefringent elements for adjustable linear coupling. We give in this paper a theoretical study of its classical and quantum properties. It is shown that two optical beams with adjustable frequencies and well-defined polarization can be emitted. The Stokes parameters of the two beams are entangled. The principal advantage of this setup is the possibility to directly generate polarization-entangled light without the need of mixing four modes on beamsplitters as required in current experimental setups. This device opens up different directions for the study of light-matter interfaces and a generation of multimode nonclassical light and higher dimensional phase space.

DOI: 10.1103/PhysRevA.73.012333 PACS number(s): 03.67.Hk, 03.67.Mn, 42.65.Yj, 42.50.Dv

I. INTRODUCTION

Developing quantum memories constitutes an essential milestone on the route towards quantum communication networks. As it is difficult to directly store photons, the quantum information has to be stored in a material-based quantum system. A particularly promising application for polarization-entangled light is the ability to couple it with atomic ensembles: the algebra describing the quantum properties of polarized light *via* Stokes operators [1–3] is exactly the same as that describing the quantum properties of the atomic spin, be it single or collective spins. Quantum state exchange between light fields and matter systems has been recently experimentally demonstrated [4,5] and it has been shown that such systems can be used as quantum memories [6]. In addition, from a technical point of view, the use of polarization states offers simpler detection schemes, without the need for local oscillators. These features make the study and experimental generation of nonclassical polarization states of first importance for continuous-variable quantum communication.

Furthermore, the study of higher dimensional phase space is a fascinating and promising subject. Indeed, it has been shown that multimode nonclassical light could be a very powerful tool for an efficient processing and transport of quantum information [7]. Already experimental implementations and applications of such nonclassical multimode light have been demonstrated in the continuous-wave regime [8–11]. Such systems either involve a very large number of modes [10,11] or a much smaller number (three in the case of Ref. [9]). Increasing the number of correlated modes is of particular importance, for instance, in the case of optical read-out technologies [12] and super-resolution techniques [13]. In this context, generating continuous-variable polarization-entangled light [1–3], which exhibits three or four mode correlations, is a first step towards increasing the phase space dimension.

Such polarization-entangled beams in the continuous-variable regime have been recently produced experimentally with injected type-I phase-matched optical parametric oscillators (OPOs) below threshold [14,15] or using $\chi^{(3)}$ effects in a cloud of cold atoms [16]. All of these methods require linear interferences of two quadrature-entangled modes with two bright coherent states, which limits the amount of entanglement reached and the simplicity and scalability of the setup.

We investigate here an approach to directly generate polarization-entangled light without the need of mode mixing. This approach stems from an original device that we previously studied, a self-phase-locked optical parametric oscillator. This system consists of a type-II phase-matched nonlinear $\chi^{(2)}$ crystal in an optical cavity and emits fields that are phase-locked through linear coupling [17–19]: a birefringent plate, which can be rotated relative to the principal axis of the crystal, adds this coupling between the orthogonally polarized signal and idler beams and results in a phase-locking phenomenon that is well known for coupled mechanical or electrical oscillators [20]. Such systems have recently attracted a lot of attention as efficient sources of nonclassical light [21–23]. A stable operation has been demonstrated experimentally even with very small coupling [17,24,25] and their nonclassical properties are very encouraging [24]. We propose here a new implementation where two crystals, and not only one, are placed with their neutral axis orthogonal in a cavity containing two birefringent waveplates for adjustable linear coupling. Each crystal generates a pair of signal and idler beams and the waveplates couple together the two signal beams and the two idler beams so that phase locking can be achieved in a nonfrequency degenerate operation. As

*Author to whom correspondence should be addressed. Email address: coudreau@spectro.jussieu.fr

we will show below, this device allows for a direct and efficient generation of polarization-entangled optical beams.

In this paper, we investigate in detail the classical and quantum properties of the system. The paper is organized as follows. In Sec. II we begin by presenting the linear and nonlinear elements of the two-crystal OPO. A propagating Jones matrix is associated with each element and permits us to access the round-trip matrix and the stationary solutions. Section III considers the quantum properties of the emitted beams in terms of quadrature operators in the Fourier domain. The usual input-output linearization technique is used and quantum correlation spectra are formulated. In Sec. IV, these quadrature correlations are then interpreted in terms of polarization entanglement through the Stokes operators. Considering various criteria, we demonstrate theoretically that this device is an efficient source of polarization entanglement.

II. SETUP AND CLASSICAL PROPERTIES

In this section, we present the basic scheme of the two-crystal OPO. Round-trip equations and stationary solutions are then derived by using Jones matrix formalism.

A. Linear and nonlinear elements in the OPO cavity

The setup is sketched in Fig. 1. Two identical type-II phase matched ($\chi^{(2)}$) crystals oriented at 90° and two birefringent waveplates are inserted inside a ring cavity. Signal and idler fields are resonant but the pump is not enhanced. The orientation of the various axes with respect to one another are critical. They are summarized on Fig. 1: the nonlinear crystals c_α and c_β have their fast axes orthogonal; waveplate l_1 has its fast axis parallel to the fast axis of the crystal c_α; the fast axis of the waveplate l_2 makes an angle ρ with respect to the fast axis of crystal c_β. In this paper, we will restrict ourselves to small values of ρ.

Four fields may propagate inside the cavity: their classical field amplitudes are denoted $a_{1,2}$ and $b_{1,2}$ where the index corresponds to the polarization and the letter to the frequency ω_a or ω_b (Fig. 1). The pump field is polarized at 45° of the crystals' axes and its amplitude is denoted a_0. We consider that the pump and subharmonic fields are coupled via the nonlinear crystals. In c_α, the phase matching is such that $a_0^{(x)}$ is coupled to a_1 and b_2 while in c_β, $a_0^{(y)}$ is coupled to a_2 and b_1.

We suppose that the waveplates for the subharmonic waves have identical dephasing for the two fields. M_1 and M_3 are highly reflective mirrors while the amplitude reflection coefficient for M_2 is denoted r. For the sake of simplicity, this coefficient is assumed to be real and independent of the frequency and of the polarization.

B. Propagation matrices

Birefringent elements are usually described by Jones matrices [26]. The total field can be decomposed into four components corresponding to the two subharmonic frequencies and the two linear polarizations. The waveplates l_1 and l_2 couple the fields a_1 and a_2, and b_1^* and b_2^* independently

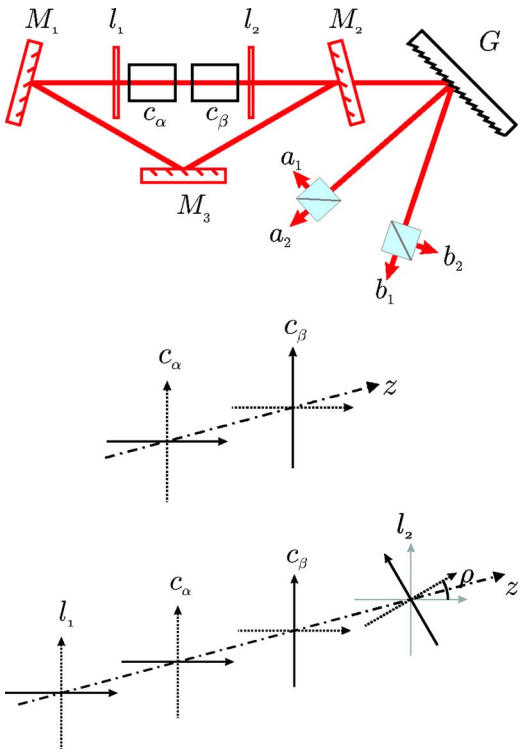

FIG. 1. (Color online) Top: Ring cavity two-crystal OPO: $c_{\alpha,\beta}$ are type-II nonlinear crystals, $l_{1,2}$ are $\lambda/2$ waveplates at $\omega_0/2$ and λ waveplates at ω_0. $M_{1,3}$ are highly reflective mirrors at $\omega_{a,b}$ and M_2 is a partially reflective mirror at $\omega_{a,b}$. All mirrors are transparent at ω_0. G is a diffraction grating which separates the two frequency components. Each of them have two orthogonally polarized bright components. Center: neutral axes seen by the fundamental wave at frequency ω_0. Bottom: neutral axes seen by the subharmonic waves at frequencies ω_1 and ω_2. Dotted lines denote fast axes and continuous lines slow axes.

while the crystals couple a_1 and b_2^*, and a_2 and b_1^* independently. Thus, the basis $\{a_1, b_2^*, a_2, b_1^*\}$ is sufficient.

The waveplate l_1 is a $\lambda/2$ with its axes parallel to the basis axes so that its associated matrix is diagonal:

$$M_{l_1} = \begin{pmatrix} ie^{ik_a ne} & 0 & 0 & 0 \\ 0 & -ie^{-ik_b ne} & 0 & 0 \\ 0 & 0 & ie^{ik_a ne} & 0 \\ 0 & 0 & 0 & -ie^{-ik_b ne} \end{pmatrix}, \quad (1)$$

where $k_{a,b}$ denotes the wave vectors, n the mean index of refraction (dispersion is neglected), and e the thickness of the plate.

To determine the transfer matrix of the nonlinear crystals, the phase matching will be taken perfect. We recall that the field amplitudes at the output of the first crystal can be written

$$a_1^{(out)} = a_1^{(in)} + g a_0^{(x)} (b_2^{(in)})^*,$$

and

$$(b_2^{(out)})^* = (b_2^{(in)})^* + g(a_0^{(x)})^*(a_1^{(in)}), \tag{2}$$

to the first order in g where $a_0^{(x)}$ denotes the pump amplitude at the output of the first crystal,

$$a_0^{(x)} = \frac{1}{\sqrt{2}} a_0, \tag{3}$$

and where g is the nonlinear coupling coefficient given by

$$g = l\chi^{(2)} \sqrt{\frac{\hbar \omega_0 \omega_a \omega_b}{2c^2 \varepsilon_0 n_0 n_1 n_2}}. \tag{4}$$

Equations (2) are only valid close to the oscillation threshold where the pump depletion is small, which corresponds to the usual operation regime of such nonlinear devices in quantum optics [24]. The transfer matrix of the first crystal takes thus the following form:

$$M_{c_\alpha} = \begin{pmatrix} e^{ik_a n_1 l} & g\frac{a_0}{\sqrt{2}} e^{ik_a n_1 l} & 0 & 0 \\ g\frac{a_0^*}{\sqrt{2}} e^{-ik_b n_2 l} & e^{-ik_b n_2 l} & 0 & 0 \\ 0 & 0 & e^{ik_a n_2 l} & 0 \\ 0 & 0 & 0 & e^{-ik_b n_1 l} \end{pmatrix}. \tag{5}$$

As stated before, perfect phase matching has been assumed. $n_{1,2}$ stand for the refractive indices along the neutral axes and l is the crystal thickness. In the second crystal, only a_2 and b_1^* are coupled to the pump. Assuming that the two crystals are at the same temperature, the transfer matrix is given by

$$M_{c_\beta} = \begin{pmatrix} e^{ik_a n_2 l} & 0 & 0 & 0 \\ 0 & e^{-ik_b n_1 l} & 0 & 0 \\ 0 & 0 & e^{ik_a n_1 l} & g a_0^{(y)} e^{ik_a n_1 l} \\ 0 & 0 & g a_0^{(y)} e^{-ik_b n_2 l} & e^{-ik_b n_2 l} \end{pmatrix}, \tag{6}$$

$a_0^{(y)}$ denotes the pump amplitude along y between the two crystals,

$$a_0^{(y)} = \frac{1}{\sqrt{2}} a_0. \tag{7}$$

Finally, the last waveplate is a $\lambda/2$ waveplate rotated by an angle $(\rho + \pi/2)$ with respect to l_1. To the first order in ρ, the transfer matrix is found to be [19]

$$M_{l_2} = \begin{pmatrix} -ie^{ik_a ne} & 0 & i\epsilon_0 e^{ik_a ne} & 0 \\ 0 & ie^{-ik_b ne} & 0 & -i\epsilon_0 e^{-ik_b ne} \\ i\epsilon_0 e^{ik_a ne} & 0 & ie^{ik_a ne} & 0 \\ 0 & -i\epsilon_0 e^{-ik_b ne} & 0 & -ie^{ik_b ne} \end{pmatrix}, \tag{8}$$

where $\epsilon_0 \equiv \sin 2\rho \approx 2\rho$.

As mentioned earlier, we assume that the mirror properties are independent both of the frequency and of the polarization. The free propagation matrix is thus

$$M_{prop} = r \begin{pmatrix} e^{ik_a L} & 0 & 0 & 0 \\ 0 & e^{-ik_b L} & 0 & 0 \\ 0 & 0 & e^{ik_a L} & 0 \\ 0 & 0 & 0 & e^{-ik_b L} \end{pmatrix}, \tag{9}$$

where L is the cavity length without taking into account the birefringent elements (waveplates and crystal).

One can now calculate the round-trip matrix:

$$M_{rt} \equiv M_{prop} \,.\, M_{l_2} \,.\, M_{c_\beta} \,.\, M_{c_{alpha}} \,.\, M_{l_1}. \tag{10}$$

Rather than giving the round-trip matrix in the general case, let us now make the following assumptions which are usually verified experimentally: the finesse for the subharmonic fields is high. The coefficient r is close to 1 and we put $r = 1 - \kappa$ with $\kappa \ll 1$; we assume that the double resonance condition is verified, that is both

$$\Delta_{a,b} = k_{a,b}[L + 2ne + l(n_1 + n_2)] \tag{11}$$

are close to an integer multiple of 2π. We denote $\delta_{a,b}$ their small round-trip phase detunings; the waveplates l_1 and l_2 are $\lambda/2$ for the two frequencies ω_a and ω_b.

In this case, the round-trip matrix to the first order in $\delta_{a,b}, g, \kappa$, and ϵ_0 takes the following form:

$$M_{rt} \approx \begin{pmatrix} 1 + i\delta_a - \kappa & g\frac{a_0}{\sqrt{2}} & \epsilon_0 & 0 \\ g\frac{a_0^*}{\sqrt{2}} & 1 - i\delta_b - \kappa & 0 & -\epsilon_0 \\ -\epsilon_0 & 0 & 1 + i\delta_a - \kappa & g\frac{a_0}{\sqrt{2}} e^{-i\psi} \\ 0 & \epsilon_0 & g\frac{a_0^*}{\sqrt{2}} e^{i\psi} & 1 - i\delta_b - \kappa \end{pmatrix}, \tag{12}$$

where $\psi = (k_b n_1 + k_a n_2) l$. The phase of the pump amplitude between the two crystals has been shifted by $(k_a + k_b) ne$.

C. Stationary solutions

The stationarity of the solutions corresponds to the fact that the field amplitudes after one round trip must be equal to the initial ones. This condition can be expressed in terms of the round-trip matrix:

$$M_{rt} \begin{pmatrix} a_1 \\ b_2^* \\ a_2 \\ b_1^* \end{pmatrix} = \begin{pmatrix} a_1 \\ b_2^* \\ a_2 \\ b_1^* \end{pmatrix}. \tag{13}$$

This system has a nontrivial solution only if

$$\det(M_{rt} - \mathbb{I}_4) = 0 \tag{14}$$

which leads to a stringent condition on the dephasings

$$\delta_a = \delta_b = \delta \tag{15}$$

and provides also an expression for the pump power $I_0^{(threshold)} = |a_0|^2$.

We will restrict ourselves to the case where $\psi=0[2\pi]$, which corresponds to the lowest threshold area. Equation (14) yields to

$$I_0^{(threshold)} = |a_0|^2 = \frac{2}{g^2}[\kappa^2 + (\delta \pm \epsilon_0)^2]. \tag{16}$$

This equation has two solutions, corresponding to two possible regimes. In this paper, we will focus on the regime of lower threshold.

These equations are similar to that obtained in a one-crystal self-phase locked OPO, which has been studied in detail in [18,19,25]. For a given input pump intensity, the phase-locked operation can be obtained only for a given range of the relevant parameters (i.e., cavity length and crystal temperature) which defines a so-called "locking zone." This locking zone is typically a cavity resonance width large in terms of length and a few kelvins in terms of temperature, well within experimental capacities. For a one-crystal self-phase-locked OPO, a phase-locked operation was indeed observed even for extremely small angles of the wave plate [24] where it does not perturb the quantum properties of the system [23].

Let us consider the lowest threshold given by Eq. (16) and reach for $\delta=\epsilon_0$. This working point, associated with $\psi=0[2\pi]$, can be obtained experimentally by simultaneously adjusting both the crystal temperatures and the frequency of the pump laser. Equation (16) becomes thus

$$I_0^{(threshold)} = 2\kappa^2/g^2. \tag{17}$$

At this working point, the round-trip matrix is simpler and can be rewritten:

$$M_{rt} = \begin{pmatrix} 1+i\epsilon_0-\kappa & \kappa & \epsilon_0 & 0 \\ \kappa & 1-i\epsilon_0-\kappa & 0 & -\epsilon_0 \\ -\epsilon_0 & 0 & 1+i\epsilon_0-\kappa & \kappa \\ 0 & \epsilon_0 & \kappa & 1-i\epsilon_0-\kappa \end{pmatrix}. \tag{18}$$

The eigenvector of the round-trip equation, $M_{rt}\vec{\mathcal{J}}=\vec{\mathcal{J}}$, is given by

$$\vec{\mathcal{J}} = \mathcal{J}\begin{pmatrix} 1 \\ 1 \\ -i \\ -i \end{pmatrix}, \tag{19}$$

where $\mathcal{J}$ is a (*a priori* complex) constant. This expression shows that the field generated consists in two modes at frequencies ω_a and ω_b with right circularly polarization. $\mathcal{J}$ is determined by the pump depletion equation:

$$a_0 = (a_0^{in} - g a_1 b_2) e^{ikn_0 l}, \tag{20}$$

where a_0^{in} is the input pump amplitude. In order to solve this equation, one can set the pump phase between the two crystals to be zero: this amounts to changing the phase origin which will not change the properties of the system. The previous equation yields

$$\left(\frac{\kappa}{g} + g|\mathcal{J}|^2\right)^2 = I_0^{(in)} \tag{21}$$

with $I_0^{(in)}=|a_0^{(in)}|^2$. One then gets the usual OPO solution

$$\mathcal{J} = \sqrt{\frac{\kappa}{g^2}(\sigma-1)}e^{i\phi_1}, \tag{22}$$

where a reduced pumping parameter σ has been defined equal to the input pump amplitude normalized to the threshold

$$\sigma = \sqrt{\frac{I_0^{(in)}}{I_0^{(threshold)}}}. \tag{23}$$

When σ is larger than 1, i.e., when the OPO is pumped above a defined threshold, four bright beams with fixed relative phases given by Eq. (19) are generated. Since the two signal (resp. idler) beams have a fixed phase relation and identical frequencies, they form a single beam with a circular polarization state. The system thus generates two circularly polarized beams which are frequency tunable.

The next sections are devoted to the study of the quantum properties. Correlations and anticorrelations of the couple signal/idler emitted by each crystal, i.e., (a_1,b_2) or (a_2,b_1), are formulated.

III. QUANTUM PROPERTIES AND QUADRATURE FLUCTUATIONS

In order to calculate the fluctuations for the involved fields when the system is pumped above threshold, we apply the usual input-output linearization technique (see, e.g., [27]). Individual noise spectra as well as the correlations between any linear combinations of the various fluctuations are derived in the Fourier domain.

A. Linearized equations

We first determine the classical stationary solutions of the evolution equations: these solutions are denoted $a_i^{(s)}$, $b_j^{(s)}$ where $i=0,1,2$; $j=1,2$. We then linearize the evolution equations around these stationary values by setting $a_i=a_i^{(s)}+\delta a_i$, $i=0,1,2$, and $b_j=b_j^{(s)}+\delta b_j, j=0,1$.

The evolution equations for the fluctuations are deduced from the round-trip matrix taking into account the stationary solutions (17), (19), and (22):

$$\tau\frac{d\delta a_1}{dt} = (-\kappa\sigma + i\epsilon_0)\delta a_1 + \kappa\delta b_2^* + e^{i\phi_1}\sqrt{\kappa(\sigma-1)}(\delta a_0^{(x)})^{(in)} + \epsilon_0\delta a_2 - e^{2i\phi_1}\kappa(\sigma-1)\delta b_2 - \sqrt{2\kappa}\delta a_1^{in},$$

$$\tau\frac{d\delta a_2}{dt} = (-\kappa\sigma + i\epsilon_0)\delta a_2 + \kappa\delta b_1^* - ie^{i\phi_1}\sqrt{\kappa(\sigma-1)}(\delta a_0^{(y)})^{(in)} - \epsilon_0\delta a_1 + e^{2i\phi_1}\kappa(\sigma-1)\delta b_1 - \sqrt{2\kappa}\delta a_2^{in},$$

$$\tau\frac{d\delta b_1}{dt} = (-\kappa\sigma + i\epsilon_0)\delta b_1 + \kappa\delta a_2^* + ie^{-i\phi_1}\sqrt{\kappa(\sigma-1)}(\delta a_0^{(y)})^{(in)} + \epsilon_0\delta b_2 + e^{-2i\phi_1}\kappa(\sigma-1)\delta a_2 - \sqrt{2\kappa}\delta b_1^{in},$$

$$\tau\frac{d\delta b_2}{dt} = (-\kappa\sigma + i\epsilon_0)\delta b_2 + \kappa\delta a_1^* - e^{-i\phi_1}\sqrt{\kappa(\sigma-1)}(\delta a_0^{(x)})^{(in)} - \epsilon_0\delta b_1 - e^{-2i\phi_1}\kappa(\sigma-1)\delta a_1 - \sqrt{2\kappa}\delta b_2^{in}, \quad (24)$$

where τ stands for the cavity round-trip time. δa_i^{in} correspond to the vacuum fluctuations entering the cavity through the coupling mirror.

B. Quadrature fluctuations

We define the amplitude and phase quadratures of a mode a with mean phase ϕ_a by, respectively,

$$p_a = \delta a e^{-i\phi_a} + \delta a^* e^{i\phi_a}, \quad q_a = -i(\delta a e^{-i\phi_a} - \delta a^* e^{i\phi_a}). \quad (25)$$

The evolution equations can be then expressed in matrix form:

$$\tau\frac{d}{dt}\delta\mathcal{J} = M\delta\mathcal{J} + \sqrt{\kappa(\sigma-1)}\delta\mathcal{J}_0^{in} + \sqrt{2\kappa}\delta\mathcal{J}^{in}, \quad (26)$$

where

$$M = \left(\begin{array}{cccc|cccc} -\kappa\sigma & -\epsilon_0 & 0 & \epsilon_0 & 0 & 0 & -\kappa(\sigma-2) & 0 \\ \epsilon_0 & -\kappa\sigma & -\epsilon_0 & 0 & 0 & 0 & 0 & -\kappa\sigma \\ 0 & \epsilon_0 & -\kappa\sigma & -\epsilon_0 & -\kappa(\sigma-2) & 0 & 0 & 0 \\ -\epsilon_0 & 0 & \epsilon_0 & -\kappa\sigma & 0 & -\kappa\sigma & 0 & 0 \\ \hline 0 & 0 & -\kappa(\sigma-2) & 0 & -\kappa\sigma & -\epsilon_0 & 0 & \epsilon_0 \\ 0 & 0 & 0 & -\kappa\sigma & \epsilon_0 & -\kappa\sigma & -\epsilon_0 & 0 \\ -\kappa(\sigma-2) & 0 & 0 & 0 & 0 & \epsilon_0 & -\kappa\sigma & -\epsilon_0 \\ 0 & -\kappa\sigma & 0 & 0 & -\epsilon_0 & 0 & \epsilon_0 & -\kappa\sigma \end{array}\right), \quad (27)$$

$\delta\mathcal{J}$ is the column vector of the quadrature components

$$\delta\mathcal{J} = (p_{a_1}, q_{a_1}, p_{a_2}, q_{a_2}, p_{b_1}, q_{b_1}, p_{b_2}, q_{b_2}), \quad (28)$$

$\delta\mathcal{J}_0^{in}$ for the input pump fluctuations,

$$\delta\mathcal{J}_0^{in} = (p_0^{(x)^{in}}, q_0^{(x)^{in}}, p_0^{(y)^{in}}, q_0^{(y)^{in}}, p_0^{(y)^{in}}, q_0^{(y)^{in}}, p_0^{(x^{in})}, q_0^{(x)^{in}}), \quad (29)$$

and $\delta\mathcal{J}^{in}$ the for the vacuum fluctuations entering the cavity through the coupling mirror

$$\delta\mathcal{J}^{in} = (p_{a_1}^{in}, q_{a_1}^{in}, p_{a_2}^{in}, q_{a_2}^{in}, p_{b_1}^{in}, q_{b_1}^{in}, p_{b_2}^{in}, q_{b_2}^{in}). \quad (30)$$

These differential equations are readily transformed into algebraic equations by taking the Fourier transform. In the frequency domain, the equations become

$$2i\Omega\delta\tilde{\mathcal{J}}(\Omega) = M'\delta\tilde{\mathcal{J}}(\Omega) + \sqrt{\frac{\sigma-1}{\kappa}}\delta\tilde{\mathcal{J}}_0^{in}(\Omega) + \sqrt{\frac{2}{\kappa}}\delta\tilde{\mathcal{J}}^{in}(\Omega), \quad (31)$$

where $\Omega = \tau\omega/2\kappa = \omega/\Omega_c$ is the noise frequency normalized to the cavity bandwidth $\Omega_c = 2\kappa/\tau$ and $c = \epsilon_0/\kappa$ is the normalized coupling constant. $\delta\tilde{\mathcal{J}}(\Omega)$, $\delta\tilde{\mathcal{J}}_0^{in}(\Omega)$, and $\delta\tilde{\mathcal{J}}^{in}(\Omega)$ are the Fourier transforms of the column vectors (28)–(30). The matrix M' is defined by

$$M' = \left(\begin{array}{cccc|cccc} -\sigma & -c & 0 & c & 0 & 0 & -\sigma-2 & 0 \\ c & -\sigma & -c & 0 & 0 & 0 & 0 & -\sigma \\ 0 & c & -\sigma & -c & -\sigma-2 & 0 & 0 & 0 \\ -c & 0 & c & -\sigma & 0 & -\sigma & 0 & 0 \\ \hline 0 & 0 & -\sigma-2 & 0 & -\sigma & -c & 0 & c \\ 0 & 0 & 0 & -\sigma & c & -\sigma & -c & 0 \\ -\sigma-2 & 0 & 0 & 0 & 0 & c & -\sigma & -c \\ 0 & -\sigma & 0 & 0 & -c & 0 & c & -\sigma \end{array}\right). \quad (32)$$

C. Correlations and anticorrelations

In order to use the symmetry of the equations, one can introduce the symmetric and antisymmetric components

$$\tilde{p}_\alpha = \frac{1}{\sqrt{2}}[\tilde{p}_{a_1}(\Omega) + \tilde{p}_{b_2}(\Omega)], \quad \tilde{q}_\alpha = \frac{1}{\sqrt{2}}[\tilde{q}_{a_1}(\Omega) + \tilde{q}_{b_2}(\Omega)],$$

$$\tilde{r}_\alpha = \frac{1}{\sqrt{2}}[\tilde{p}_{a_1}(\Omega) - \tilde{p}_{b_2}(\Omega)], \quad \tilde{s}_\alpha = \frac{1}{\sqrt{2}}[\tilde{q}_{a_1}(\Omega) - \tilde{q}_{b_2}(\Omega)], \tag{33}$$

and

$$\tilde{p}_\beta = \frac{1}{\sqrt{2}}[\tilde{p}_{a_2}(\Omega) + \tilde{p}_{b_1}(\Omega)], \quad \tilde{q}_\beta = \frac{1}{\sqrt{2}}[\tilde{q}_{a_2}(\Omega) + \tilde{q}_{b_1}(\Omega)],$$

$$\tilde{r}_\beta = -\frac{1}{\sqrt{2}}[\tilde{p}_{a_2}(\Omega) - \tilde{p}_{b_1}(\Omega)], \quad \tilde{s}_\beta = -\frac{1}{\sqrt{2}}[\tilde{q}_{a_2}(\Omega) - \tilde{q}_{b_1}(\Omega)]. \tag{34}$$

In a standard OPO, one expects intensity correlations and phase anticorrelations. Using our notations, this corresponds to having r_α and r_β as well as q_α and q_β squeezed [28]. This is also the case in a phase-locked OPO in the limit of small coupling [23].

As previously, the equations verified by these quantities can be expressed in matrix form. However, it is interesting to note that the sums are independent from the differences. Thus, one can write two sets of equations:

$$2i\Omega\,\delta\tilde{w}_\pm(\Omega) = M_\pm \delta\tilde{w}_\pm(\Omega) + \sqrt{2\frac{\sigma-1}{\kappa}}\,\delta\tilde{w}^{in}_{0,\pm}(\Omega) + \sqrt{\frac{2}{\kappa}}\,\delta\tilde{w}^{in}_{\pm}(\Omega), \tag{35}$$

where $\delta\tilde{w}_\pm$ are the column vector

$$\delta\tilde{w}_+(\Omega) = (\tilde{p}_\alpha(\Omega), \tilde{p}_\beta(\Omega), \tilde{q}_\alpha(\Omega), \tilde{q}_\beta(\Omega)),$$

$$\delta\tilde{w}_-(\Omega) = (\tilde{r}_\alpha(\Omega), \tilde{r}_\beta(\Omega), \tilde{s}_\alpha(\Omega), \tilde{s}_\beta(\Omega)), \tag{36}$$

$$M_+ = \begin{pmatrix} -2(\sigma-1) & 0 & -c & c \\ 0 & -2(\sigma-1) & c & -c \\ c & -c & -2\sigma & 0 \\ -c & c & 0 & -2\sigma \end{pmatrix},$$

$$M_- = \begin{pmatrix} -2 & 0 & -c & -c \\ 0 & -2 & -c & -c \\ c & c & 0 & 0 \\ c & c & 0 & 0 \end{pmatrix}, \tag{37}$$

$\delta\tilde{w}^{in}_{0,\pm}$ are the column vectors for the input pump fluctuations,

$$\delta\tilde{w}^{in}_{0,+} = (\tilde{p}_0^{(x)in}(\Omega), \tilde{p}_0^{(y)in}(\Omega), \tilde{q}_0^{(x)in}(\Omega), \tilde{p}_0^{(y)in}(\Omega)),$$

$$\delta\tilde{w}^{in}_{0,-} = (0,0,0,0), \tag{38}$$

and $\delta\tilde{w}^{in}$ the column vector for the input fluctuations entering the cavity through the coupling mirror

$$\delta\tilde{w}^{in}_+(\Omega) = (\tilde{p}^{in}_\alpha(\Omega), \tilde{p}^{in}_\beta(\Omega), \tilde{q}^{in}_\alpha(\Omega), \tilde{q}^{in}_\beta(\Omega))$$

$$\delta\tilde{w}^{in}_-(\Omega) = (\tilde{r}^{in}_\alpha(\Omega), \tilde{r}^{in}_\beta(\Omega), \tilde{s}^{in}_\alpha(\Omega), \tilde{s}^{in}_\beta(\Omega)). \tag{39}$$

These equations can be easily solved and one obtains the equations for the intracavity fluctuations. However, the relevant fluctuations are those outside the cavity. They can be easily calculated using the boundary condition on the output mirror:

$$f_{out} = tf - rf_{in} \approx \sqrt{2\kappa} f - f_{in} \tag{40}$$

and the corresponding spectra are given by

$$\mathcal{S}_f(\Omega) = \langle \tilde{f}_{out}(\Omega)\tilde{f}^*_{out}(-\Omega)\rangle. \tag{41}$$

The expressions are identical for the two sets of spectra $\mathcal{S}_{p_\alpha,q_\alpha,r_\alpha,s_\alpha}$ and $\mathcal{S}_{p_\beta,q_\beta,r_\beta,s_\beta}$:

$$\mathcal{S}_{p_u}(\Omega) = 1 + \frac{1}{2[\Omega^2 + (\sigma-1)^2]} + \frac{\sigma^2 + \Omega^2 - c^2}{2\{[c^2 + \sigma(\sigma-1)]^2 + \Omega^2 - 2[c^2 - \sigma(\sigma-1)]\Omega^2 + \Omega^4\}},$$

$$\mathcal{S}_{q_u}(\Omega) = 1 - \frac{1}{\Omega^2 + \sigma^2} - \frac{(\sigma-1)^2 + \Omega^2 - c^2}{2\{[c^2 + \sigma(\sigma-1)]^2 + \Omega^2 - 2[c^2 - \sigma(\sigma-1)]\Omega^2 + \Omega^4\}},$$

$$\mathcal{S}_{r_u}(\Omega) = 1 - \frac{1}{2(1+\Omega^2)} - \frac{\Omega^2 - c^2}{2[\Omega^2 + (\Omega^2 - c^2)^2]},$$

$$\mathcal{S}_{s_u}(\Omega) = 1 + \frac{1}{2\Omega^2} + \frac{1 + \Omega^2 - c^2}{2[\Omega^2 + (\Omega^2 - c^2)^2]}, \tag{42}$$

$u = \alpha, \beta$.

The behavior of the squeezed spectra, $\mathcal{S}_{r_u^{(out)}}$ and $\mathcal{S}_{q_u^{(out)}}$, is shown in Fig. 2. For small coupling and low analysis frequency, one observes that the spectra go to zero which indicates the existence of very large correlations. As usual, the spectra go to 1 as Ω goes to infinity: the correlations exist only within the cavity bandwidth or conversely, only when the integration time is larger than the field life time in the cavity. The increase of c also results in a degradation of the correlations and anticorrelations: the waveplate tends to mix the fields, and this phenomenon is increased as the coupling is increased. This phenomenon can be understood in terms of phase diffusion: as the coupling is increased, the phase diffusion is reduced which in turn reduces the intensity correlations. Finally, the phase anticorrelations (Fig. 2, bottom) are also degraded as the input pump power is increased: as σ

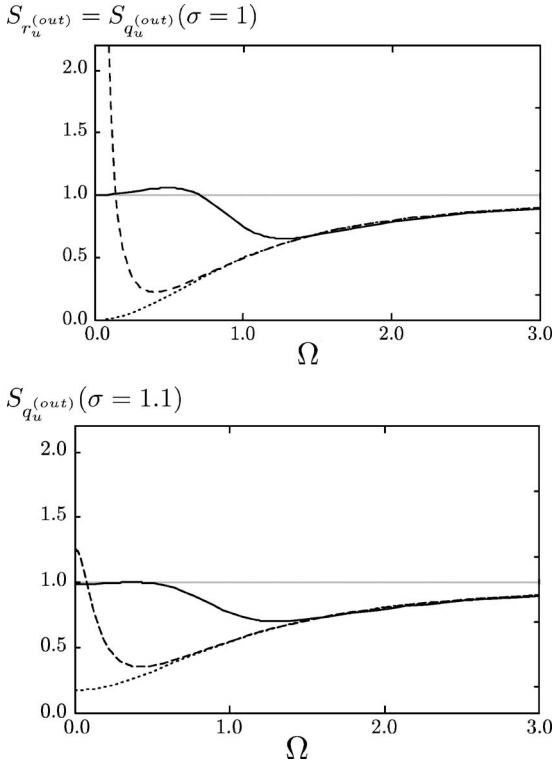

FIG. 2. Normalized noise spectrum of the amplitude quadrature difference and phase quadrature sum for $\sigma=1$ (top) and $\sigma=1.1$ (bottom). Continuous curves corresponds to $c=1$, long-dashed to $c=0.2$, and short-dashed to $c=0$.

is increased, the input pump noise becomes more and more important.

This analysis has been performed by studying the fields generated by each crystal. Since several frequencies are involved, such a measurement would require the use of multiple local oscillators or of dephasing cavities [29]. It is thus easier experimentally as well as more fruitful for quantum information purposes to study the beams at each frequency, namely the couples (a_1,a_2) and (b_1,b_2), which are circularly polarized.

IV. POLARIZATION-ENTANGLEMENT GENERATION

The nonclassical properties of the two-crystal OPO are now analyzed in terms of polarization fluctuations. Polarization-entanglement generation is demonstrated using various criteria introduced in the literature.

A. Quantum Stokes parameters

Before describing the properties of the system, let us briefly recall the quantum picture for polarization properties. The polarization of light beams can be described in the general case by the Stokes parameters [30]:

$$S_0 = I_x + I_y, \quad S_1 = I_x - I_y,$$

$$S_2 = I_{+45^\circ} - I_{-45^\circ}, \quad S_3 = I_{\sigma^+} - I_{\sigma^-}. \tag{43}$$

where $I_{x,y,+45^\circ,-45^\circ,\sigma^+,\sigma^-}$ describe the intensity along the x, y, $+45^\circ$, -45°, σ^+, and σ^- polarization. These four parameters are not independent but are instead linked by the relation

$$S_0^2 = S_1^2 + S_2^2 + S_3^2 \tag{44}$$

for a totally polarized field.

The quantum polarization properties are defined via the quantum counterparts of the Stokes parameters [1,2]:

$$\hat{S}_0 = \hat{a}_x^\dagger \hat{a}_x + \hat{a}_y^\dagger \hat{a}_y, \quad \hat{S}_1 = \hat{a}_x^\dagger \hat{a}_x - \hat{a}_y^\dagger \hat{a}_y,$$

$$\hat{S}_2 = \hat{a}_x^\dagger \hat{a}_y + \hat{a}_y^\dagger \hat{a}_x = \hat{a}_{+45^\circ}^\dagger \hat{a}_{+45^\circ} + \hat{a}_{-45^\circ}^\dagger \hat{a}_{-45^\circ},$$

$$\hat{S}_3 = i(\hat{a}_y^\dagger \hat{a}_x - \hat{a}_x^\dagger \hat{a}_y) = \hat{a}_{\sigma^+}^\dagger \hat{a}_{\sigma^+} + \hat{a}_{\sigma^-}^\dagger \hat{a}_{\sigma^-}. \tag{45}$$

$(\hat{S}_1,\hat{S}_2,\hat{S}_3)$ verify commutation relations identical to those verified by orbital momentum operators:

$$[\hat{S}_i,\hat{S}_j] = 2i\hat{S}_k, \tag{46}$$

where $i,j,k=1,2,3$ are cyclically interchangeable. These relations result in three uncertainty relations,

$$\Delta^2\hat{S}_1\Delta^2\hat{S}_2 \geqslant |\langle \hat{S}_3\rangle|^2, \quad \Delta^2\hat{S}_2\Delta^2\hat{S}_3 \geqslant |\langle \hat{S}_1\rangle|^2,$$

$$\Delta^2\hat{S}_3\Delta^2\hat{S}_1 \geqslant |\langle \hat{S}_2\rangle|^2, \tag{47}$$

where the notation $\Delta^2(\hat{X})$ correspond to the variance of the operator $\hat{X}$.

B. Entanglement criteria

In our case, Eq. (19) shows that the output beams are circularly polarized, thus $\langle \hat{S}_1^{a,b}\rangle = 0 = \langle \hat{S}_2^{a,b}\rangle$; and as a result, the inequalities (47) which contain variances $\hat{S}_3^{a,b}$ are automatically verified. The only nontrivial Heisenberg inequality is then given by

$$\Delta^2\hat{S}_1^{a,b}\Delta^2\hat{S}_2^{a,b} \geqslant |\langle \hat{S}_3^{a,b}\rangle|^2 = \frac{\kappa}{g^2}(\sigma - 1), \tag{48}$$

where the notation $\Delta^2(\hat{X})$ corresponds to the variance of the operator $\hat{X}$: $\Delta^2(\hat{X}) = \langle (\hat{X} - \langle \hat{X}\rangle)^2\rangle = \langle \delta X^2\rangle$.

Various entanglement criteria have been defined. We will restrict ourselves to three of them [31–34].

The first two criteria are, in the general case, sufficient (and not always necessary) conditions for entanglement. A general criterion is given by the product of two linear combinations of conjugate variables variances [33] (denoted "product criterion" in the following). In the case of the Stokes operators, this inseparability criterion states that when

$$\Delta^2(\hat{S}_1^a \pm \hat{S}_1^b)\Delta^2(\hat{S}_2^a \mp \hat{S}_2^b) \leqslant 2(|\langle \hat{S}_3^a\rangle| + |\langle \hat{S}_3^b\rangle|) \tag{49}$$

the state is entangled. The relevant Stokes parameters fluctuations $\delta\hat{S}_1^{a,b}$ and $\delta\hat{S}_2^{a,b}$ can be expressed from the quadrature operators. In the case of circularly polarized beams, one has $(u=a,b)$

$$\frac{\delta\hat{S}_1^u(\Omega)}{|\mathcal{J}|} = \delta\bar{p}_{u_1}^{(out)}(\Omega) - \delta\bar{p}_{u_2}^{(out)}(\Omega),$$

$$\frac{\delta\hat{S}_2^u(\Omega)}{|\mathcal{J}|} = -[\delta\tilde{q}_{u_1}^{(out)}(\Omega) - \delta\tilde{q}_{u_2}^{(out)}(\Omega)]. \tag{50}$$

It follows from these expressions that

$$\begin{aligned}\delta S_1^+ &= \delta\hat{S}_1^a(\Omega) + \delta\hat{S}_1^b(\Omega)\\ &= [\delta\tilde{p}_{a_1}^{(out)}(\Omega) - \delta\tilde{p}_{b_2}^{(out)}(\Omega)] - [\delta\tilde{p}_{a_2}^{(out)}(\Omega) - \delta\tilde{p}_{b_1}^{(out)}(\Omega)]\\ &= \sqrt{2}(r_\alpha^{(out)} - r_\beta^{(out)}),\end{aligned}$$

$$\begin{aligned}\delta S_2^- &= \delta\hat{S}_2^a(\Omega) - \delta\hat{S}_2^b(\Omega)\\ &= -[\delta\tilde{q}_{a_1}^{(out)}(\Omega) + \delta\tilde{q}_{b_2}^{(out)}(\Omega)] + [\delta\tilde{q}_{a_2}^{(out)}(\Omega) + \delta\tilde{p}_{b_1}^{(out)}(\Omega)]\\ &= \sqrt{2}(-q_\alpha^{(out)} + q_\beta^{(out)}).\end{aligned} \tag{51}$$

Thus the relevant spectra can be calculated from the previously calculated linear combinations of the amplitude and phase quadrature components. They are given by

$$\mathcal{S}_{S_1^+}(\Omega) = 1 - \frac{\Omega^2 - c^2}{\Omega^2 + (\Omega^2 - c^2)^2},$$

$$\begin{aligned}&\mathcal{S}_{S_2^-}(\Omega)\\ &\quad = 1 - \frac{(\Omega^2 - c^2) + (\sigma - 1)^2}{[c^2 + \sigma(\sigma - 1)]^2 + \Omega^2 - 2[c^2 - \sigma(\sigma - 1)]\Omega^2 + \Omega^4}.\end{aligned} \tag{52}$$

Let us remark that the two expressions are equal for $\sigma = 1$ and $c = 0$, i.e., for the uncoupled system operated at threshold. One also remarks that $\mathcal{S}_{S_1^+}(\Omega)$ is independent of the pump amplitude σ. This is not surprising since this quantity is the difference of the intensity correlations between the signal and idler modes of each crystal. These correlations originate in the parametric down-conversion phenomenon, independently of the pump power: the photons in the modes a_1 and b_2 (a_2 and b_1, respectively) are emitted by pairs thus leading to intensity correlations between the two modes. These two quantities can be measured using standard methods for the measurement of quantum Stokes operators, see, e.g., [2,14,15]

Using these expressions, one gets a simple expression for the product criterion (49)

$$\mathcal{S}_{S_1^+}(\Omega)\mathcal{S}_{S_2^-}(\Omega) \leqslant 2. \tag{53}$$

The second criterion ("sum criterion"), which is widely used in continuous-variable entanglement characterization, is given by the sum of the above quantities [31,32]. It is, in fact, a special case of the previous criterion [33]. The criterion states that if

$$\frac{1}{2}(\mathcal{S}_{S_1^+} + \mathcal{S}_{S_2^-}) \leqslant 1 \tag{54}$$

then the two states are entangled.

These two criteria are entanglement witnesses in the sense that they allow us to specify whether the state is indeed entangled.

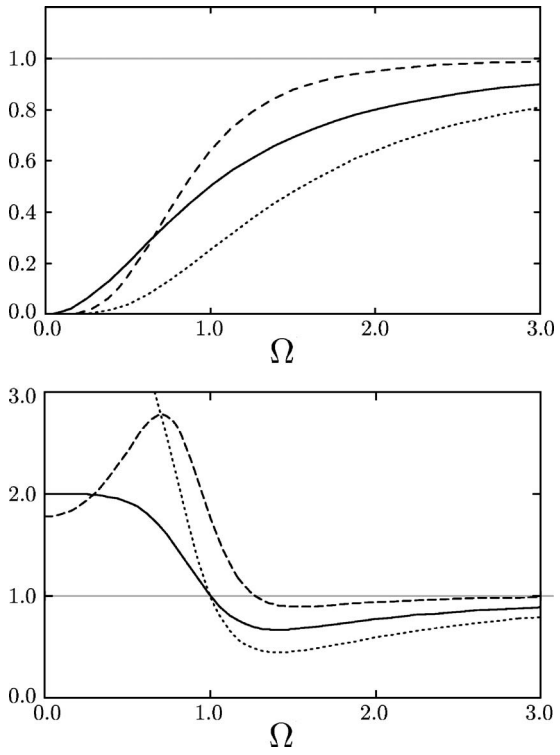

FIG. 3. Criterion spectra for $c=0$ (top) and $c=1$ (bottom). Continuous curves correspond to the sum criterion $\left[\frac{1}{2}\mathcal{S}_{S_1^+}(\Omega) + \mathcal{S}_{S_2^-}(\Omega)\right]$, long-dashed to the EPR criterion $(\mathcal{S}_{S_1^a|S_1^b}.\mathcal{S}_{S_2^a|S_2^b})$, and short-dashed to the product criterion $\left[\frac{1}{2}(\mathcal{S}_{S_1^+}.\mathcal{S}_{S_2^-})\right]$.

Finally, the last criterion is related to another particularity of the system which may allow us to make a joint QND measurement of the two noncommutating observables $\hat{S}_1$ and $\hat{S}_2$. It is shown in [34] that this is related to the EPR-like "paradox." This criterion relies on conditional probabilities and can be written

$$\mathcal{S}_{S_1^a|S_1^b}.\,\mathcal{S}_{S_2^a|S_2^b} \leqslant 1, \tag{55}$$

where

$$\mathcal{S}_{S_i^a|S_i^b} = \langle (S_i^a)^2\rangle\left(1 - \frac{\langle S_i^a S_i^b\rangle^2}{\langle (S_i^a)^2\rangle\langle (S_i^b)^2\rangle}\right), \quad i = 1,2. \tag{56}$$

When this condition is verified, the correlations are sufficiently large that the information extracted from the measurement of the two Stokes operators of one field provides values for the Stokes operators of the other which violate the Heisenberg inequality [35].

Figure 3 shows the various criteria as a function of the analysis frequency, Ω for a fixed pump power ($\sigma=1$) and for different values of the coupling. Very strong entanglement can be found for small couplings, c and small analysis frequencies Ω. As the coupling is increased, the entanglement is shifted to higher values of the analysis frequency. Let us note, however, that $c=1$ corresponds usually to large angles (around 1° for typical output couplers): in the case of single-crystal phase locked OPOs, stable phase-locking has been

achieved with very small angles corresponding to $c \approx 0$. The entanglement is present for a wide range of the parameters thus showing the efficiency of the system.

V. CONCLUSION

We have presented and studied theoretically an original device based on an optical cavity containing two type-II phase-matched $\chi^{(2)}$ crystals as well as birefringent plates which add a linear coupling between the signal and idler fields emitted in each crystal. The coupling induces a phase-locking, respectively, between the two signal fields and between the two idler fields. In this configuration, the system is found to directly generate two-color polarization-entangled beams without the need for mode mixing. The two-crystal OPO would be thus a useful resource for the field of continuous-variable quantum information. Nonclassical polarization states are well coupled to atomic ensembles which can be used as quantum memories and form the basic block required for quantum networks. Furthermore, we believe that the experimental implementation of this device is very interesting for potential parallel processing as it would be a new step towards extending the dimension of the phase space experimentally accessible.

ACKNOWLEDGMENTS

Laboratoire Kastler-Brossel of the Ecole Normale Supérieure and the Université Pierre et Marie Curie, is associated with the Centre National de la Recherche Scientifique (UMR 8552). Laboratoire Matériaux et Phénomènes Quantiques of Université Denis Diderot, is associated with the Centre National de la Recherche Scientifique (UMR 7162). We thank A. Gatti for pointing us to Ref. [33] and acknowledge fruitful discussions with G. Adesso and A. Serafini.

[1] A. S. Chirkin, A. A. Orlov, and D. Yu Parschuk, Kvantovaya Elektron. (Moscow) **20**, 999 (1993) [Quantum Electron. **23**, 870 (1993)].
[2] N. Korolkova, G. Leuchs, R. Loudon, T. C. Ralph, and C. Silberhorn, Phys. Rev. A **65**, 052306 (2002).
[3] N. Korolkova and R. Loudon, Phys. Rev. A **71**, 032343 (2005).
[4] B. Julsgaard, J. Sherson, J. I. Cirac, J. Fiurasek, and E. S. Polzik, Nature (London) **432**, 482 (2004).
[5] M. D. Lukin, Rev. Mod. Phys. **75**, 457 (2003).
[6] A. Dantan, A. Bramati, and M. Pinard, Europhys. Lett. **67**, 881 (2004).
[7] A. Gatti, I. V. Sokolov, M. I. Kolobov, and L. A. Lugiato, Eur. Phys. J. D **30**, 123 (2004).
[8] M. Martinelli, N. Treps, S. Ducci, S. Gigan, A. Maître, and C. Fabre, Phys. Rev. A **67**, 023808 (2003).
[9] N. Treps, N. Grosse, W. P. Bowen, C. Fabre, H. A. Bachor, and P. K. Lam, Science **940**, 940 (2003).
[10] O. Jedrkiewicz, Y.-K. Jiang, E. Brambilla, A. Gatti, M. Bache, L. A. Lugiato, and P. Di Trapani, Phys. Rev. Lett. **93**, 243601 (2004).
[11] A. Mosset, F. Devaux, and E. Lantz, Phys. Rev. Lett. **94**, 223603 (2005).
[12] V. Delaubert, N. Treps, G. Bo, and C. Fabre, eprint quant-ph/0512152.
[13] V. N. Beskrovnyy and M. I. Kolobov, Phys. Rev. A **71**, 043802 (2005).
[14] W. P. Bowen, N. Treps, R. Schnabel, and P. K. Lam, Phys. Rev. Lett. **89**, 253601 (2002).
[15] R. Schnabel, W. P. Bowen, N. Treps, T. Ralph, H. A. Bachor, and P. K. Lam, Phys. Rev. A **67**, 012316 (2003).
[16] V. Josse, A. Dantan, A. Bramati, and E. Giacobino, J. Opt. B: Quantum Semiclassical Opt. **6**, S532 (2004).
[17] E. J. Mason and N. C. Wong, Opt. Lett. **23**, 1733 (1998).
[18] C. Fabre, E. J. Mason, and N. C. Wong, Opt. Commun. **170**, 299 (1999).
[19] L. Longchambon, J. Laurat, T. Coudreau, and C. Fabre, Eur. Phys. J. D **30**, 279 (2004).
[20] A. Pikovsky, M. Rosenblum, and J. Kurths, *Synchronization* (Cambridge University Press, Cambridge, England, 2001).
[21] L. Longchambon, J. Laurat, N. Treps, S. Ducci, A. Maître, T. Coudreau, and C. Fabre, J. Phys. I **12**, Pr5-147 (2002).
[22] H. H. Adamyan and G. Yu. Kryuchkyan, Phys. Rev. A **69**, 053814 (2004).
[23] L. Longchambon, J. Laurat, T. Coudreau, and C. Fabre, Eur. Phys. J. D **30**, 287 (2004).
[24] J. Laurat, T. Coudreau, L. Longchambon, and C. Fabre, Opt. Lett. **30**, 1177 (2005).
[25] P. Groß, K.-J. Boller, and M. E. Klein, Phys. Rev. A **71**, 043824 (2005).
[26] R. C. Jones, J. Opt. Soc. Am. **31**, 488 (1941).
[27] C. Fabre, E. Giacobino, A. Heidmann, L. Lugiato, S. Reynaud, M. Vadacchino, and W. Kaige, Quantum Opt. **2**, 159 (1990).
[28] S. Reynaud, C. Fabre, and E. Giacobino, J. Opt. Soc. Am. B **4**, 1520 (1987).
[29] A. S. Villar, L. S. Cruz, K. N. Cassemiro, M. Martinelli, and P. Nussenzveig, Phys. Rev. Lett. **95**, 24 3603 (2005).
[30] G. G. Stokes, Trans. Cambridge Philos. Soc. **9**, 399 (1852).
[31] Lu-Ming Duan, G. Giedke, J. I. Cirac, and P. Zoller, Phys. Rev. Lett. **84**, 2722 (2000).
[32] R. Simon, Phys. Rev. Lett. **84**, 2726 (2000).
[33] V. Giovannetti, S. Mancini, D. Vitali, and P. Tombesi, Phys. Rev. A **67**, 022320 (2003).
[34] M. D. Reid and P. Drummond, Phys. Rev. Lett. **60**, 2731 (1988).
[35] N. Treps and C. Fabre, Laser Phys. **15**, 187 (2005).